
PHYSICO-CHEMICAL STUDIES
OF SYSTEMS AND PROCESSES

Synthesis and Electrical Properties of Ternary Molybdates $\text{Li}_3\text{Ba}_2\text{R}_3(\text{MoO}_4)_8$ (R = La–Lu, Y)

N. M. Kozhevnikova and O. A. Kopylova

*Baikal Institute of Nature Management, Siberian Branch, Russian Academy of Sciences,
Ulan-Ude, Buryatia, Russia*

Received May 17, 2010

Abstract—X-ray diffraction and differential-thermal analyses were used to study the phase relations in the subsolidus region of the system $\text{Li}_2\text{MoO}_4\text{–BaMoO}_4\text{–R}_2(\text{MoO}_4)_3$. The temperature dependence of the conductivity of $\text{Li}_3\text{Ba}_2\text{R}_3(\text{MoO}_4)_8$ phases (R = Y, Eu, Sm, La) was examined.

DOI: 10.1134/S1070427211030086

The keen interest in representatives of oxide phases crystallizing in NASICON and sheelite structural types is due to their unique properties: high chemical and thermal stability, low thermal expansion, and high ionic conductivity.

Molybdates with a sheelite structure are promising materials for various electric devices, batteries, and sensors, which is associated with the high mobility of lithium, sodium, and silver cations due to the specific sheelite-like structure of molybdates and tungstates.

In [1, 2], the phase formation in the subsolidus region of the systems $\text{Me}_2\text{MoO}_4\text{–AMoO}_4\text{–R}(\text{MoO}_4)$ (R = La–Lu, Y) was studied, and ternary molybdates with NASICON and sheelite structure were obtained. It was demonstrated that, with increasing radius of the R^{3+} cation in the octahedral coordination, the mobility of the alkali cation grows, which leads to a rise in the ionic conductivity of the phases.

It is of interest to examine a new group of ternary molybdates containing cations of lithium, barium, and rare-earth elements. The presence of three cations in the structure of molybdates enables control over the mobility of cations.

The goal of our study was to synthesize the ternary molybdates $\text{Li}_3\text{Ba}_2\text{R}_3(\text{MoO}_4)_8$, to subject these compounds to X-ray and differential-thermal analyses, and to examine the nature of their conductivity.

EXPERIMENTAL

As starting components for a study of the phase formation in the systems $\text{Li}_2\text{MoO}_4\text{–BaMoO}_4\text{–R}_2(\text{MoO}_4)_3$ served Li_2MoO_4 , BaMoO_4 , and $\text{R}_2(\text{MoO}_4)_3$ preliminarily synthesized by the solid-phase method from Li_2CO_3 , BaO , R_2O_3 , and MoO_3 . We studied the interaction in the systems $\text{Li}_2\text{MoO}_4\text{–BaMoO}_4\text{–R}_2(\text{MoO}_4)_3$ in two stages. First, we examined the phase composition at intersections of the sections emerging from middle and double molybdates formed in the boundary binary systems $\text{Li}_2\text{MoO}_4\text{–R}_2(\text{MoO}_4)_3$ and $\text{BaMoO}_4\text{–R}_2(\text{MoO}_4)_3$, with the system $\text{Li}_2\text{MoO}_4\text{–Ba}(\text{MoO}_4)_2$ being eutectic. In the second stage, we examined the revealed quasibinary sections, which enabled triangulation of the systems.

We studied in most detail (in steps of 1–2 mol %) the interaction in the $\text{BaMoO}_4\text{–LiR}(\text{MoO}_4)_2$ section. It was found that, for the whole series of rare-earth elements, including yttrium, ternary molybdates $\text{Li}_3\text{Ba}_2\text{R}_3(\text{MoO}_4)_8$ are formed at 650–700°C. The samples were annealed at 400, 500, 550, 600, and 650°C, with multiple intermittent grindings after every 20–30 h. The time of calcination at each temperature was 100–120 h. On being annealed, the samples were gradually cooled with the furnace. Nonequilibrium samples were additionally annealed; the equilibrium was considered to be attained if the phase composition of the samples remained the same after two successive annealings. The synthesis products were identified by

Crystallographic parameters of ternary molybdates

| Compound | Unit cell parameters | | | | $V/z, \text{\AA}$ |
|---|----------------------|---------------------|----------------------|---------------------|-------------------|
| | $\alpha, \text{\AA}$ | $\beta, \text{\AA}$ | $\gamma, \text{\AA}$ | β, deg | |
| $\text{Li}_3\text{Ba}_2\text{La}_3(\text{MoO}_4)_8$ | 5.343(1) | 12.963(2) | 19.304(3) | 91.26(2) | 668.3 |
| $\text{Li}_3\text{Ba}_2\text{Ce}_3(\text{MoO}_4)_8$ | 5.333(3) | 12.941(2) | 19.281(2) | 91.12(3) | 665.8 |
| $\text{Li}_3\text{Ba}_2\text{Pr}_3(\text{MoO}_4)_8$ | 5.272(2) | 12.875(3) | 19.252(5) | 91.34(1) | 653.2 |
| $\text{Li}_3\text{Ba}_2\text{Nd}_3(\text{MoO}_4)_8$ | 5.251(2) | 12.308(4) | 19.236(7) | 91.17(2) | 646.8 |
| $\text{Li}_3\text{Ba}_2\text{Sm}_3(\text{MoO}_4)_8$ | 5.247(1) | 12.794(3) | 19.202(4) | 91.29(2) | 664.3 |
| $\text{Li}_3\text{Ba}_2\text{Eu}_3(\text{MoO}_4)_8$ | 5.241(1) | 12.775(2) | 19.185(4) | 91.18(2) | 642.2 |
| $\text{Li}_3\text{Ba}_2\text{Gd}_3(\text{MoO}_4)_8$ | 5.238(5) | 12.758(2) | 19.151(2) | 91.13(3) | 639.7 |
| $\text{Li}_3\text{Ba}_2\text{Tb}_3(\text{MoO}_4)_8$ | 5.230(2) | 12.746(2) | 19.122(4) | 91.41(2) | 637.2 |
| $\text{Li}_3\text{Ba}_2\text{Ho}_3(\text{MoO}_4)_8$ | 5.209(2) | 12.705(2) | 19.112(2) | 91.44(2) | 632.2 |
| $\text{Li}_3\text{Ba}_2\text{Dy}_3(\text{MoO}_4)_8$ | 5.222(2) | 12.717(2) | 19.117(3) | 91.37(2) | 634.6 |
| $\text{Li}_3\text{Ba}_2\text{Er}_3(\text{MoO}_4)_8$ | 5.181(2) | 12.673(3) | 19.105(4) | 91.53(1) | 626.8 |
| $\text{Li}_3\text{Ba}_2\text{Tm}_3(\text{MoO}_4)_8$ | 5.180(5) | 12.614(1) | 19.057(2) | 91.42(3) | 622.4 |
| $\text{Li}_3\text{Ba}_2\text{Yb}_3(\text{MoO}_4)_8$ | 5.115(3) | 12.609(4) | 19.100(6) | 91.51(2) | 615.7 |
| $\text{Li}_3\text{Ba}_2\text{Lu}_3(\text{MoO}_4)_8$ | 5.002(1) | 12.544(2) | 19.097(2) | 91.63(4) | 598.9 |
| $\text{Li}_3\text{Ba}_2\text{Y}_3(\text{MoO}_4)_8$ | 5.189(3) | 12.694(4) | 19.109(5) | 91.57(2) | 629.1 |

X-ray phase analysis (XPA). X-ray diffraction patterns of the samples were measured in an FR-552 chamber-monochromator ($\text{CuK}\alpha$ radiation, Ge as internal standard). The X-ray powder diffraction patterns were analyzed with an IZA-2 comparator.

The diffraction patterns were processed using the Rentgen standard software package. The differential-thermal analysis (DTA) was made with an MOM OD-

103 derivatograph (Hungary) at a heating rate of 10 deg min^{-1} , with 0.3–0.4-g samples.

The temperature dependences of the conductivity σ , dielectric constant ϵ , and dielectric loss tangent $\tan \sigma$ were studied using the Vest-Tallan polarization technique on densely compacted ceramic samples having the form of pellets 10 mm in diameter and

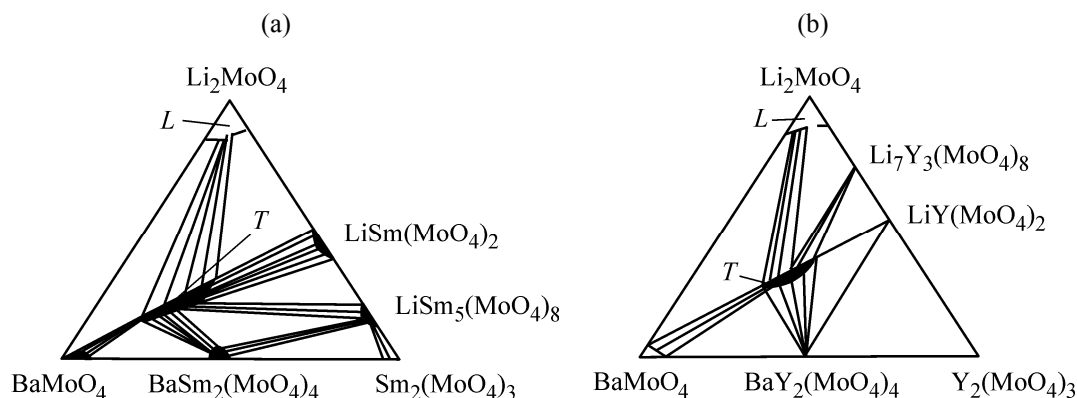


Fig. 1. Phase relations (at 700°C) in the systems (a) $\text{Li}_2\text{MoO}_4\text{--BaMoO}_4\text{--Sm}_2(\text{MoO}_4)_3$ and (b) $\text{Li}_2\text{MoO}_4\text{--BaMoO}_4\text{--Y}_2(\text{MoO}_4)_3$. T : (a) $\text{Li}_3\text{Ba}_2\text{Sm}_3(\text{MoO}_4)_8$ and (b) $\text{Li}_3\text{Ba}_2\text{Y}_3(\text{MoO}_4)_8$.

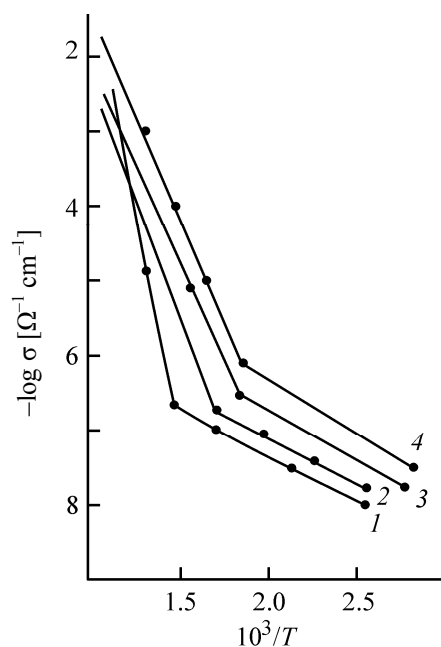


Fig. 2. Dependence of the electrical conductivity σ on the temperature T , K. (1) $\text{Li}_3\text{Ba}_2\text{Y}_3(\text{MoO}_4)_8$, (2) $\text{Li}_3\text{Ba}_2\text{Eu}_3(\text{MoO}_4)_8$, (3) $\text{Li}_3\text{Ba}_2\text{Sm}_3(\text{MoO}_4)_8$, and (4) $\text{Li}_3\text{Ba}_2\text{La}_3(\text{MoO}_4)_8$.

1–1.5 mm thick, with platinum electrodes. The electrodes were deposited by brazing a platinum paste.

The electrical properties were measured with an E8-4 ac bridge at a frequency of 103 Hz. A P-5025 capacitance box was used, which extended the range in which the dielectric loss tangent could be measured (determination accuracy $\pm 5\%$).

The dc current was measured with an E6-13A teraohmmeter at a voltage of 30–50 mV.

The reproducibility of measurement results was verified under heating and cooling in the temperature range 20–600°C. The sample temperatures were measured in the course of our electrical studies with a chromel–alumel thermocouple connected to a V7-21A voltmeter, with an accuracy of $\pm 2^\circ$.

As regards the nature of phase transformations, the systems under study can be divided into two groups: (1) $R = \text{La}–\text{Tb}$ and (2) $R = \text{Dy}–\text{Lu}$, Y, which is due to the different phase compositions of the boundary systems $\text{Li}_2\text{MoO}_4–\text{R}_2(\text{MoO}_4)_3$. For the systems with $R = \text{La}–\text{Tb}$, the quasibinary sections are $\text{Li}_2\text{MoO}_4–\text{Li}_3\text{Ba}_2\text{R}_3(\text{MoO}_4)_8$, $\text{BaMoO}_4–\text{Li}_3\text{Ba}_2\text{R}_3(\text{MoO}_4)_8$, $\text{BaR}_2(\text{MoO}_4)_4–\text{Li}_3\text{Ba}_2\text{R}_3(\text{MoO}_4)_8$, $\text{BaR}_2(\text{MoO}_4)_4–\text{LiR}_5(\text{MoO}_4)_8$, $\text{Li}_3\text{Ba}_2\text{R}_3(\text{MoO}_4)_8–\text{LiR}_5(\text{MoO}_4)_8$, and $\text{Li}_3\text{Ba}_2\text{R}_3(\text{MoO}_4)_8–\text{LiR}(\text{MoO}_4)_2$ (Fig. 1a). In the systems of the second

group ($R = \text{Dy}–\text{Lu}$, Y), the phase equilibria at 700°C are characterized by the following quasibinary sections: $\text{Li}_2\text{MoO}_4–\text{Li}_3\text{Ba}_2\text{R}_3(\text{MoO}_4)_8$, $\text{Li}_7\text{R}_3(\text{MoO}_4)_8–\text{Li}_3\text{Ba}_2\text{R}_3(\text{MoO}_4)_8$, $\text{BaMoO}_4–\text{Li}_3\text{Ba}_2\text{R}_3(\text{MoO}_4)_8$, $\text{Li}_3\text{Ba}_2\text{R}_3(\text{MoO}_4)_8–\text{LiR}(\text{MoO}_4)_2$, $\text{Li}_3\text{Ba}_2\text{R}_3(\text{MoO}_4)_8–\text{BaR}_2(\text{MoO}_4)_4$, and $\text{BaR}_2(\text{MoO}_4)_4–\text{LiR}(\text{MoO}_4)_2$ (Fig. 1b). $\text{Li}_3\text{Ba}_2\text{R}_3(\text{MoO}_4)_8$ incongruently melt in the temperature range 920–1015°C without undergoing any polymorphic transformations.

According to X-ray diffraction data, the lithium–barium–rare-earth molybdates $\text{Li}_3\text{Ba}_2\text{R}_3(\text{MoO}_4)_8$ belong to the structural type of a monoclinically distorted sheelite, sp.gr. $C2/c$, $Z = 2$. The compounds are isostructural with each other and with double molybdates $\text{BaR}_2(\text{MoO}_4)_4$ ($R = \text{Ce}–\text{Dy}$ [1, 4]). The structure of these latter is constituted by honeycomb-like layers of R-octagons, with Mo-tetrahedra connected to both sides of a layer via common oxygen vertices. Lithium atoms occupy different crystallographic positions in the structure of the prototype $\text{BaR}_2(\text{MoO}_4)_4$, one third of lithium atoms are statistically situated in positions of the rare-earth element with a coordination number $CN = 8$. The remaining two thirds of lithium atoms are localized in a partial position on a second-order axis, with octahedral coordination with respect to oxygen. In this case, these positions are occupied in an ordered or partially ordered way, which does not lead to a new superstructure, although a new structure does appear. A variant of the cation distribution among crystallographic positions (leading to $D_0 = 2.10\%$) was taken into account when we derived the crystallographic formula of the compounds $\text{Li}_2(\text{Ba}_{0.85}\text{R}_{0.15})_2(\text{R}_{0.675}\text{Ba}_{0.075}\text{Li}_{0.25})_4(\text{MoO}_4)_8$.

The crystallographic parameters of $\text{Li}_3\text{Ba}_2\text{R}_3(\text{MoO}_4)_8$ are listed in the table. The unit cell volumes of the phases steadily decrease in the order La–Lu, which is due to manifestation of the “lanthanide” contraction in the series of rare-earth elements.

The conductivity of the ternary molybdates $\text{Li}_3\text{Ba}_2\text{R}_3(\text{MoO}_4)_8$ varies within the range from 10^{-8} to $10^{-2} \Omega^{-1} \text{cm}^{-1}$ as temperature increases from 20 to 500°C, with the conductivity mostly having ionic nature ($t_i = 0.82–0.87$). The temperature dependences of σ are characterized by a single break, which probably corresponds to transition from impurity conductivity to that of the intrinsic type (Fig. 2).

The conductivity of up to $10^{-2} \Omega^{-1} \text{cm}^{-1}$ is due to the rather large size of rare-earth ions and voids in the sheelite-like skeleton, which substantially reduces the

steric hindrance to the transport of lithium ions. In the temperature range 20–600°C, the dielectric constant ϵ varies from 120 to 600, and the dielectric loss tangent, from 2.5 to 13.

The high ionic conductivity of the ternary molybdates $\text{Li}_3\text{Ba}_2\text{R}_3(\text{MoO}_4)_8$ enables their use as solid electrolytes with conduction by lithium ions.

CONCLUSIONS

(1) Ternary molybdates of composition $\text{Li}_3\text{Ba}_2\text{R}_3(\text{MoO}_4)_8$ (R = La–Lu, Y) were produced by the method of solid-phase reactions in the system $\text{Li}_2\text{MoO}_4\text{–BaMoO}_4\text{–R}_2(\text{MoO}_4)_3$.

(2) It was demonstrated by means of an X-ray diffraction analysis that the ternary molybdates $\text{Li}_3\text{Ba}_2\text{R}_3(\text{MoO}_4)_8$ belongs to the structural type of a monoclinically distorted sheelite, sp.gr. C2/c, $Z = 2$.

The compounds are isostructural with each other and with the binary molybdates $\text{BaR}_2(\text{MoO}_4)_4$, where R = Ce–Dy.

(3) The compounds have a predominantly ionic conductivity.

REFERENCES

1. Kozhevnikova, N.M. and Mokhosoev, M.V., *Troinye molibdaty* (Ternary Molybdates), Ulan-Ude: Buryat. Gos. Univ., 2000.
2. Kozhevnikova, N.M., Korsun, V.P., Mursakhanova, I.I., and Mokhosoev, M.V., *J. Rare Earth, Proc. 2nd Int. Conf. on Rare Earth Development and Application*, 1991, vol. 2, pp. 845–849.
3. Vest, R.V. and Tallan, V.H., *J. Appl. Phys.*, 1965, vol. 36, no. 2, pp. 547–552.
4. Kiseleva, I.I., Sirota, M.I., Ozerov, R.P., et al., *Kristallografiya*, 1979, vol. 24, no. 6, pp. 1277–1281.